Applied Physics Letters

Nonvolatile organic bistable devices fabricated utilizing Cu_2O nanocrystals embedded in a polyimide layer

Cite as: Appl. Phys. Lett. **89**, 122110 (2006); https://doi.org/10.1063/1.2355465
Submitted: 08 February 2006 • Accepted: 05 August 2006 • Published Online: 20 September 2006

Jae Hun Jung, Jae-Ho Kim, Tae Whan Kim, et al.

Nonvolatile organic bistable devices fabricated utilizing Cu_2O nanocrystals embedded in a polyimide layer

Jae Hun Jung, Jae-Ho Kim, and Tae Whan Kim[a)]
Advanced Semiconductor Research Center, Division of Electronics and Computer Engineering, Hanyang University, Seoul 133-791, Korea

Mun Seop Song and Young-Ho Kim
Division of Materials Science and Engineering, Hanyang University, Seoul 133-791, Korea

Sungho Jin
Materials Science and Engineering Program, University of California at San Diego, La Jolla, California 92093-0411

(Received 8 February 2006; accepted 5 August 2006; published online 20 September 2006)

The bistable effects of cuprous oxide (Cu_2O) nanoparticles embedded in a polyimide (PI) matrix were investigated. Transmission electron microscopy images and selected area electron diffraction patterns showed that Cu_2O nanocrystals were formed inside the PI layer. Current-voltage (*I-V*) measurements on Al/PI/nanocrystalline Cu_2O/PI/Al structures at 300 K showed a nonvolatile electrical bistability behavior. A bistable behavior for the fabricated organic bistable device (OBD) structures is described on the basis of the *I-V* results. These results indicate that OBDs fabricated utilizing self-assembled inorganic Cu_2O nanocrystals embedded in an organic PI layer hold promise for potential applications in nonvolatile flash memory devices. © *2006 American Institute of Physics*. [DOI: 10.1063/1.2355465]

Nanoparticles have been useful for fabrication and applications of electronic and optoelectronic devices operating at lower currents and higher temperatures.[1–5] Three-dimensionally confined nanoparticles embedded in insulating layers have been investigated extensively for their promising applications in nonvolatile flash memory devices with nanoscale floating gates.[6–11] Among the several types of memory devices, organic bistable devices (OBDs) consisting of organic/metal/organic structure sandwiched between two metal electrodes are attractive and promising candidates for next-generation nonvolatile flash memories,[12–18] especially due to their relatively simple fabrication techniques involved. While there are some recent reports of metal nanoclusters embedded in conducting organic layers for OBD-type applications,[19,20] research works on either fabrication or mechanism of OBDs made of self-assembled semiconductor nanoparticles have not yet been reported.

This letter reports on nonvolatile OBDs utilizing chemically self-assembled, uniformly distributed cuprous oxide (Cu_2O) semiconductor nanoparticles in polyimide (PI) matrix. The unique nonvolatile electrical bistability properties of the OBDs are discussed. Transmission electron microscopy (TEM) and selected area electron diffraction pattern (SADP) analysis were carried out to investigate the microstructural nature of the Cu_2O nanoparticles embedded in the PI layer. Current-voltage (*I-V*) measurements were carried out to investigate the properties of the electrical fabricated OBDs containing Cu_2O nanoparticles.

The samples used in this study were grown on Al-coated glass substrates by using a selective chemical reaction in the Cu film while the polyimide precursor was being cured by heating. The PI precursor used in this experiment was prepared by dissolving *p*-phenylene biphenyltetracarboximide (BPDA-PDA), a type of polyamic acid (PI2610D, Dupont), in *N*-methyl-2-pyrrolidone (1:3 ratio by weight). The BPDA-PDA solution was then spin coated onto a glass substrate. The PI precursor was subsequently soft baked at 135 °C for 30 min in order to evaporate away the solvent. Subsequently, a 5-nm-thick Cu film was deposited on the PI-precursor-coated substrate by using a thermal evaporator. Stacked thin films were cured at 350 °C for 2 h in a N_2 atmosphere in order to polymerize the polyamic acid into the PI. The formation of the Cu_2O nanoparticles embedded in the PI layer was confirmed by the absorbance, photoluminescence, and SADP measurements. The detailed growth process and the formation mechanism of the Cu_2O nanoparticles embedded in the PI layer are described elsewhere.[21,22] The PI/Cu_2O/PI/SiO_2/*n*-Si samples were also prepared for TEM analysis to prove the formation of the Cu_2O nanocrystals, and Al/PI/Al/glass samples were fabricated as a base structure to compare the electrical properties with those of the Al/PI/Cu_2O/PI/Al/glass OBD structure.

TEM observations were performed in a JEM 2010 JEOL transmission electron microscope operating at 200 kV. The *I-V* measurements were performed by using an HP 4284A precision LCR meter at 300 K.

Figure 1 shows (a) plane-view and (b) cross-sectional bright-field TEM images of the Cu_2O nanoparticles embedded in a PI matrix cured at 350 °C for 2 h. The plane-view bright-field TEM image shows that the Cu_2O nanoparticles embedded in the PI layer are relatively uniformly distributed. The size of the nanoparticles varies slightly between approximately 3 and 4 nm, and the surface density of the nanoparticles is estimated to be $\sim 2.7 \times 10^{12}$ particles/cm^2. The cross-sectional bright-field TEM image, Fig. 1(b), clearly indicates that the Cu_2O nanoparticles are fully embedded within the PI matrix. The typical diameter of the Cu_2O nanoparticles is ~4–5 nm, and this result is in a reasonable

[a)]Author to whom correspondence should be addressed; electronic mail: twk@hanyang.ac.kr

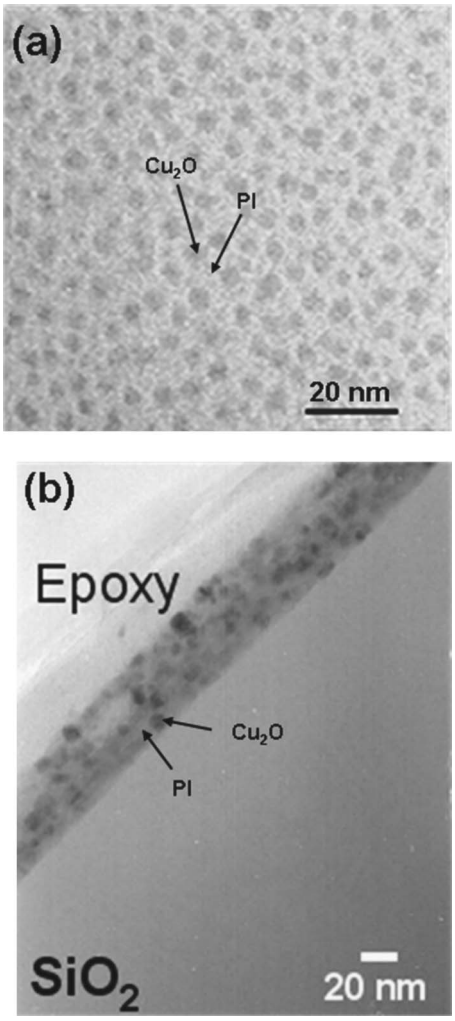

FIG. 1. (a) Plane-view and (b) cross-sectional bright-field transmission electron microscopy images of Cu_2O nanoparticles embedded in a polyimide layer cured at 350 °C for 2 h.

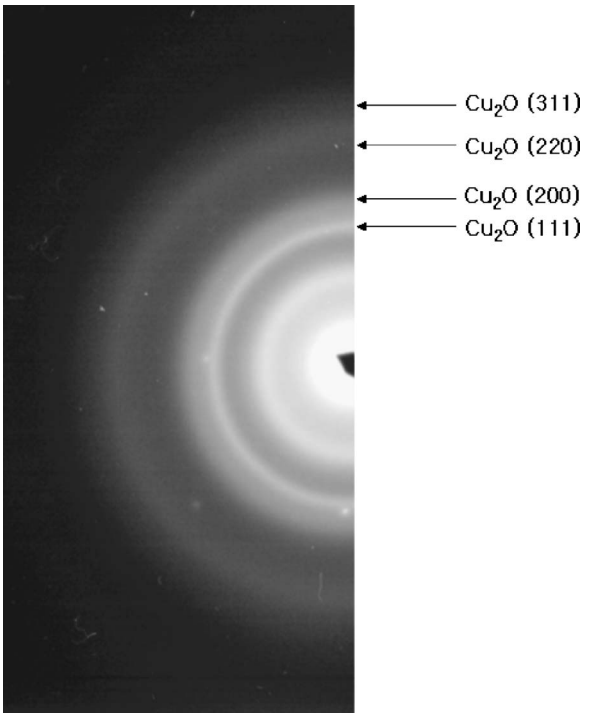

FIG. 2. Selected area electron diffraction pattern of the Cu_2O nanoparticles embedded in a polyimide layer cured at 350 °C for 2 h.

agreement with the plane-view bright-field TEM measurements of Fig. 1(a).

Figure 2 shows the SADP of the Cu_2O nanoparticles in the PI, which is indexed as a face-centered cubic crystal structure and has diffuse rings due to the small particle size. This result indicates that the Cu_2O nanoparticles precipitated and embedded in the PI layer have been crystallized. The presence of Cu_2O nanocrystals is clarified by using absorbance and PL measurements. However, the possibility of the existence of the pure Cu nanoparticles cannot be totally removed.

The organic bistable memory device was constructed by sequential addition, on a glass wafer substrate, of an aluminum (Al) electrode (100 nm thick), a PI insulating layer, a Cu_2O-embedded PI layer (~40 nm thick), another PI insulator layer, and finally an Al electrode layer. The *I-V* curves for the Al/PI (20 nm)/Cu_2O nanocrystal/PI (20 nm)/Al/glass OBD measured from +30 to −30 V and then from −30 to +30 V are shown in Fig. 3 as the curves with filled and the open circles, respectively. The state "1" and the state "0" correspond to the relatively high current and the low current states, respectively. Figure 3 clearly shows an electrical hysteresis behavior which is an essential feature for a bistable device. The bistable behavior is asymmetric, which may originate from the nonuniformity distribution of the carriers existing at the subband in the Cu_2O nanocrystals embedded in the PI layer or from the existence of interface traps between the PI layer and the Al electrodes. The exact reason for the asymmetric behavior is not clearly understood at present, and a further research is required to understand the nature of such a phenomenon. The characteristics presented by the curves can be explained in terms of two states and four stages. In a given voltage range, the curve with the lower current represents the state 0, and the curve with the higher current represents the state 1. Stages 1, 2, 3, and 4 correspond to changes in voltage from 30 to 0 V, from 0 to −30 V, from −30 to 0 V, and from 0 to 30 V, respectively. The observation that the OBD maintains state 1 in the applied voltage range from 0 to −30 V (stage 2) is similar to that reported in Ref. 14 in an Al/AIDCN organic/Al-nanocluster/AIDCN organic/Al system.

The transition from stage 2 to stage 3 (state 1 to state 0) at −30 V (considered as the V_{write}) is equivalent to the writing process in a digital memory cell.[13] The current difference between stage 2 (state 1) and stage 3 (state 0) is maximum at −10 V (considered as the V_{read}), which is equivalent to a reading process in a digital memory cell. Similarly, the current difference between stage 1 (state 0) and stage 4 (state 1) is maximum at 10 V (considered as the V_{erase}), which is equivalent to an erase process in a digital memory cell. Again, a similar behavior was reported in Ref. 14 for a different structure consisting of AIDCN organic/Al-nanocluster/AIDCN organic materials. Since the current difference between the two states under negative applied voltages is larger than that under positive applied voltages, the writing and the reading processes in the OBD structure are performed at negative voltages, and the erasing procedure is carried out at positive voltages. Even though the current difference of 2 decades might be barely enough for applications in memory devices, the magnitudes of the maximum and the minimum

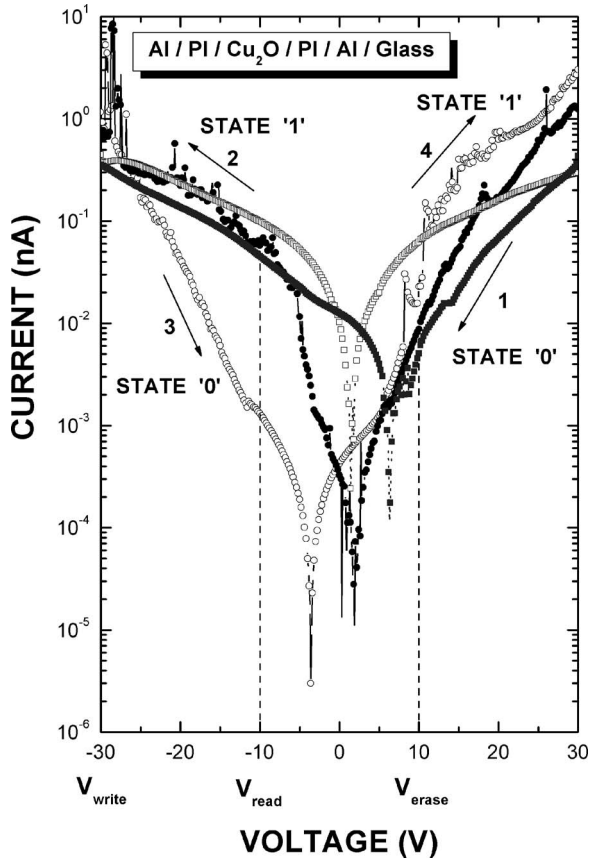

FIG. 3. Current-voltage curve for an Al/polyimide/Cu_2O nanocrystal/polyimide/Al/glass structure (circles) and an Al/polyimide/Al/glass structure (rectangles) measured from +30 to −30 V (filled) and from −30 to +30 V (open).

voltages should be decreased for fabricating high-efficiency devices.

The *I-V* curves under forward and reverse bias voltages depict the electrical bistability of the OBD structure and describe the nonvolatile nature of the memory effect.[14] Since the magnitude of the hysteresis of the *I-V* curve for the sample with the embedded Cu_2O nanocrystals is much larger than that in the Cu_2O-free sample under identical measurement conditions, as shown in Fig. 3, the OBDs fabricated utilizing embedded self-assembled Cu_2O nanocrystals exhibit a significantly enhanced information storage capability, and thus hold a promise for potential applications in nonvolatile flash memories.

Even though the nonvolatile electrical bistability behavior of the Cu_2O-containing OBD appears to be somewhat complicated, the bistable mechanism for the OBD can be surmised on the basis of the *I-V* results. The free electrons injected from the Al electrode to the PI layer are partly captured by the ground electronic subband of the Cu_2O nanocrystals embedded in the PI layer, resulting in the formation of a negatively trapped charge space near the electron injecting contact.[23] When the electrons are captured by the ground electronic subband of the Cu_2O nanocrystals embedded in the PI layer, an internal electric field is induced by the captured electrons, resulting in a decrease in the conductivity of the OBDs containing Cu_2O nanoparticles.

In summary, chemically self-assembled, mutually separated Cu_2O nanocrystals embedded in a polyimide matrix were fabricated. TEM analysis showed that Cu_2O nanocrystals were formed within the PI layer. The *I-V* curves at ambient temperature for the Al/PI/Cu_2O nanocrystal/PI/Al OBDs exhibited a nonvolatile electrical bistable behavior. A bistable behavior for the fabricated OBD structures was proposed based on the *I-V* curve characteristics. Even though systematic investigations concerning the read and write methods and the critical memory parameters for the memory devices remain to be clarified, these results indicate that the Cu_2O nanocrystal based, OBDs are easy to fabricate and hold a promise for potential applications in next-generation nonvolatile flash memory devices.

This work was supported by the National Research Program for the 0.1 Terabit Non-Volatile Memory Development sponsored by Korea Ministry of Commerce, Industry and Energy. One of the authors (J.H.J.) was supported by the Seoul Science Fellowship.

[1] X. F. Duan and C. M. Lieber, Adv. Mater. (Weinheim, Ger.) **12**, 298 (2000).
[2] R. J. Warburton, C. Schaflein, D. Haft, F. Bickel, A. Lorke, K. Karrai, J. M. Garcia, W. Schoenfeld, and P. M. Petroff, Nature (London) **405**, 926 (2000).
[3] B. H. Kind, H. Yan, B. Messer, M. Law, and P. Yang, Adv. Mater. (Weinheim, Ger.) **14**, 158 (2002).
[4] N. J. Craig, J. M. Taylor, E. A. Lester, C. M. Marcus, M. P. Hanson, and A. C. Gossard, Science **304**, 565 (2004).
[5] J. H. Kim, J. Y. Jin, J. H. Jung, I. Lee, T. W. Kim, Sung K. Lim, C. S. Yoon, and Y.-H. Kim, Appl. Phys. Lett. **86**, 032904 (2005).
[6] M. Saitoh, E. Nagata, and T. Hiramoto, Appl. Phys. Lett. **82**, 1787 (2003).
[7] M. Perego, S. Ferrari, M. Fanciulli, G. Ben Assayag, C. Bonafos, M. Carrada, and A. Claverie, J. Appl. Phys. **95**, 257 (2004).
[8] E. Kapetanakis, P. Normand, D. Tsoukalas, and K. Beltsios, Appl. Phys. Lett. **80**, 2794 (2002).
[9] T. W. Kim, D. C. Choo, J. H. Shim, and S. O. Kang, Appl. Phys. Lett. **80**, 2168 (2002).
[10] A. Kanjilal, J. Lundsgaard Hansen, P. Gaiduk, A. Nylandsted Larsen, N. Cherkashin, A. Claverie, P. Normand, E. Kapelanakis, D. Skarlatos, and D. Tsoukalas, Appl. Phys. Lett. **82**, 1212 (2003).
[11] M. Kanoun, A. Souifi, T. Baron, and F. Mazon, Appl. Phys. Lett. **84**, 5079 (2004).
[12] L. P. Ma, J. Liu, S. M. Pyo, and Y. Yang, Appl. Phys. Lett. **80**, 362 (2002).
[13] L. P. Ma, J. Liu, and Y. Yang, Appl. Phys. Lett. **80**, 2997 (2002).
[14] L. P. Ma, S. M. Pyo, J. Y. Ouyang, Q. Y. Xu, and Y. Yang, Appl. Phys. Lett. **82**, 1419 (2003).
[15] J. H. Wu, L. P. Ma, and Y. Yang, Phys. Rev. B **69**, 115321 (2004).
[16] L. D. Bozano, B. W. Kean, V. R. Deline, J. R. Salem, and J. C. Scott, Appl. Phys. Lett. **84**, 607 (2004).
[17] D. Tondelier, K. Kmimouni, D. Vuillaume, C. Fery, and G. Hass, Appl. Phys. Lett. **85**, 5763 (2004).
[18] T. Oyamada, H. Tanaka, K. Matsushige, H. Sasabe, and C. Adachi, Appl. Phys. Lett. **83**, 1252 (2003).
[19] J. Y. Ouyang, C.-W. Chu, C. R. Szmanda, L. P. Ma, and Y. Yang, Nat. Mater. **3**, 918 (2004).
[20] J. Y. Ouyang, C.-W. Chu, D. Sieves, and Y. Yang, Appl. Phys. Lett. **86**, 123507 (2005).
[21] Y.-H. Kim, G. F. Walker, J. Kim, and J. Park, J. Adhes. Sci. Technol. **1**, 331 (1987).
[22] Y. Chung, H. P. Park, H. J. Jeon, C. S. Yoon, Sung K. Kim, and Y.-H. Kim, J. Vac. Sci. Technol. B **21**, L9 (2003).
[23] N. R. Tu and K. C. Kao, J. Appl. Phys. **85**, 7267 (1999).